Penerbit Akademia Baru

Journal of Advanced Research in Experimental Fluid Mechanics and Heat Transfer

http://www.akademiabaru.com/submit/index.php/arefmht
ISSN: 2756-8202

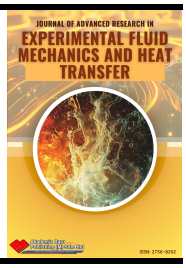

An Investigation into the Potential Capabilities of a YSZ-SDCC Composite Electrolyte for Intermediate Temperature Solid Oxide Fuel Cells

Nurul Farhana Abdul Rahman[1], Mohammad Haziq Mohammed Sofi[1], Hamimah Abd. Rahman[1,*], Umira Asyikin Md Yusop[1], Mohd Azham Azmi[1], Tan Kang Huai[2], Mohamed Abdelghani Elsayed Abdelghani Elshaikh[3]

[1] Faculty of Mechanical and Manufacturing Engineering, Universiti Tun Hussein Onn Malaysia, 86400 Batu Pahat, Johor, Malaysia
[2] Department of Materials Engineering, Faculty of Engineering and Technology, Tunku Abdul Rahman University of Management and Technology, Jalan Genting Kelang, Setapak, 53300, Kuala Lumpur, Malaysia
[3] Faculty of Mechanical Engineering, Islamic University of Madinah, Prince Naif Ibn Abdulazil, Al Jamiah, Medina, Kingdom of Saudi Arabia

ABSTRACT

The development and analysis of Yttria-Stabilized Zirconia-Samarium-Doped Ceria Carbonate (YSZ-SDCC) composite electrolytes that are intended for use in Solid Oxide Fuel Cells (ITSOFC) at intermediate temperatures is the primary focus of this study, which represents a significant advancement in the technology of SOFC. When it comes to assessing the efficiency of fuel cells, which is a strategy that shows promise for the conversion of energy, the electrolyte material is one of the most significant components that must be considered. In this study, several different compositions of YSZ-SDCC composite electrolytes were investigated in detail. Electrochemical impedance spectroscopy, often known as EIS, was applied in order to carry out a thorough investigation into the conductivity and area-specific resistance (ASR) of these composite electrolytes. This investigation covered a temperature range from 500 ℃ to 700 ℃. Several other techniques, including XRD, FTIR, FESEM, and EDS, were applied to explore the chemical compatibility of these YSZ-SDCC composite electrolytes and to analyse the microstructure characteristics of these electrolytes. Additionally, the percentage of the pellet's porosity was also calculated. YSZ-SDCC composite electrolyte with a composition ratio of 50:50 wt.% exhibits the lowest total polarization resistance (*Rp*) of 13.24 Ω at 700℃ with 9.0 x 10^{-3} Scm^{-1} ionic conductivity. These findings indicate that a YSZ-SDCC composite electrolyte with a 50:50 wt.% has a promising potential for future research due to the high conductivity resulting from the presence of strong electrolytes that produce many ions.

Keywords:
Composite electrolyte performance; intermediate temperature; ionic conductivity; performance evaluation; SOFC

Received: 25 November 2024 | **Revised: 12 December 2024** | **Accepted: 15 December 2024** | **Published: 31 December 2024**

1. Introduction

A fuel cell system generates electricity and water with enhanced efficiency while producing nearly zero emissions [1]. One of the fuel cells is solid oxide fuel cells (SOFC), which have garnered increased attention and attractiveness as a potentially useful power technology for the next generation. Compared to other types of fuel cells, SOFC technology has been deemed to be the most reliable and

* *Corresponding author.*
E-mail address: hamimah@uthm.edu.my

https://doi.org/10.37934/arefmht.18.1.1425

efficient. SOFC has several benefits, including its high energy efficiency, its adaptability to fuel, and its capacity to employ non-precious metals with electrode components [2]. SOFC is an electrochemical device that uses ion-conducting ceramic membranes to transform gaseous fuel into electrical energy. Common gases, such as hydrogen, natural gas, and biogas, were the primary fuel for SOFC [3]. When discussing the working principle of SOFC, water (H_2O) is generated as a result of the reaction with hydrogen. As a consequence of this, the products that are generated are heat, water, and electricity [4]. SOFC places a strong emphasis on its solid build where a single SOFC cell consists of two porous electrodes, referred to as cathode and anode, with a dense electrolyte layer dividing them. The anode of a SOFC is the negative terminal where oxygen ions from the electrolyte combine with fuel, producing electrons that flow into the external circuit [4]. The cathode component of the SOFC acts as the positive terminal, where oxygen molecules from the air are converted into oxygen ions by gaining electrons from the external circuit [4]. Additionally, the electrolyte layer serves as the central component of the SOFC, which is responsible for conducting electricity through the free movement of oxygen ions [5,6].

SOFCs function at high temperatures, usually ranging from 800℃ to 1,000 ℃ to enable effective fuel-to-electricity conversion [7]. The high working temperature allows for the utilization of different fuels and the recovery of excess heat for increased power production [8]. As a consequence of this, the cost of manufacturing and operating the SOFC is excessively high, despite the fact that the cell's overall lifespan is limited [9]. One effective approach to enhancing the sustained durability, stability, and reducing production costs of SOFC systems is by lowering their operating temperature to below 800℃ [10]. On a side note, lowering the operating temperatures could result in degradation of cell performance. Improving cell performance at low temperatures can be accomplished by developing new materials or enhancing current materials [11].

The high ionic conductivity of YSZ makes it a popular solid electrolyte material for use in SOFC. Yttria dopant stabilizes zirconia's cubic and tetragonal structure at high and low temperatures. However, dopant yttria concentration affects cell conductivity. Fergus *et al.,* [12] discovered that cell conductivity increases with yttria dopant concentration, although the composition must not exceed 8.0 mol% Y_2O_3. SDC has been widely utilized in numerous research studies because of its outstanding ionic conductivity, stability, and compatibility [13,14]. Regrettably, doped ceria may experience mixed ionic and electronic conduction (MIEC) issues, resulting in a decrease in cell performance. It was discovered that ceria possesses a fluorite type crystal structure, which is not ideal for conducting oxygen when utilized as MIEC materials [15]. Introducing salts or hydrates like chlorides, fluorites, carbonate, and sulphates as a secondary phase into doped ceria has the potential to enhance ionic conductivity [16,17]. These salts have shown proton conduction, which aligns with oxygen ion conduction.

The investigation of Yttria-stabilized zirconia (YSZ) and samarium-doped ceria (SDC) carbonates aimed to identify an effective solution for enhancing electrolyte performance. To achieve this, electrochemical impedance spectroscopy (EIS) was employed to perform a thorough analysis of the conductivity and area-specific resistance (ASR) of these composite electrolytes within a temperature range of 500°C to 700°C. Additionally, various advanced characterization techniques were used to assess the chemical compatibility and microstructural properties of the YSZ-SDC composite electrolytes. X-ray diffraction (XRD) was utilized to examine the crystalline structure, Fourier-transform infrared spectroscopy (FTIR) provided insights into functional groups and bonding, field emission scanning electron microscopy (FESEM) was employed to observe surface morphology and detailed microstructural features, and energy-dispersive X-ray spectroscopy (EDS) was used to determine elemental composition. In addition, the porosity percentage of the pellets was determined to provide a thorough grasp of the material's characteristics.

2. Methodology

2.1 Preparation of YSZ-SDCC Composite Electrolyte Powder and Characterization of the Powder

A composite powder of SDCC was prepared using wet ball milling method with 80 wt.% of SDC (KCeracell Co. Ltd. Korea) raw powder and 20 wt.% of binary carbonates (Li_2CO_3 and Na_2CO_3). The molar ratios of Li_2CO_3 and Na_2CO_3 (Sigma Aldrich, USA) were 67:33 [18]. The SDCC slurry was dried at 90°C for 12 hours and the dried SDCC was crushed in an agate mortar to form a fine powder. The powder was heated to 680°C and maintained at that temperature for an hour, with a heating and cooling rate of 5°C/min. Following that, commercial powder YSZ (KCeracell Co. Ltd. Korea) was mixed with prepared SDCC composite powder at three different compositions by using high speed ball milling method. The milled YSZ-SDCC wet mixes were dried and calcined. Table 1 shows the compositions of the prepared YSZ-SDCC composite electrolytes powders. Prior research on the NiO-SDCC composite and SSC-SDCC composite influenced the selection of the composition ratio for YSZ-SDCC [19,20].

YSZ-SDCC composite electrolytes powder were analysed for phase identification using X-ray diffraction (XRD) machine (Brucker D8 Advance, Germany). The analysis was conducted with Cu Kα emission radiation at a wavelength of 0.15418 nm (λ=0.15418) and a scanning range of 2θ from 20° to 80°. The crystalline phase of all the powders was analysed to verify a pure crystalline structure without any contamination or presence of a second phase. Fourier transform infrared spectroscopy (FTIR) (Perkin Elmer Spectrum 100, USA) was implemented to identify the potential presence of carbonates that may remain following the extensive milling procedure. Next, the microstructure and element composition distribution were analysed using field-emission scanning electron microscopy (FESEM) with electron-dispersive spectroscopy (EDS; JSM 6380-Jeol, Japan).

Table 1
Weight ratio composition (wt.%) of YSZ-SDCC composite electrolytes powders

Electrolytes composite powders	Weight ratio composition (wt.%)	Designated samples
YSZ-SDCC	50:50	YSC55
YSZ-SDCC	60:40	YSC64
YSZ-SDCC	70:30	YSC73

2.2 Electrochemical Performances of YSZ-SDCC Symmetrical Cell

The uniaxial pressing method was used to press the pellet samples for the YSZ-SDCC composite electrolyte powder. This approach is compatible with prepared powders and is easy to manage. A 0.5g powder is compressed using uniaxial pressing with 1 ton of pressure applied. The pellets were sintered at 680°C for one hour with a controlled heating and cooling rate of 5°C/min. The YSZ-SDCC pellets were coated on both sides with silver conductive paste after sintering procedure. The 8 pellets with a silver paste coating were dried in an oven at 135°C to ensure the adherence and stability of the conductive layers. A 1 mm thick and 13 mm diameter YSZ-SDCC symmetrical cell was fabricated and subsequently evaluated for its electrochemical performance. Electrochemical Impedance Spectroscopy (EIS) was utilized to assess the conductivity and area specific resistance (ASR) for all the fabricated YSZ-SDCC samples at 500℃, 600℃ and 700℃.

The electrochemical performance of YSC55, YSC64, and YSC73 was evaluated within the temperature range of 700℃ to 50℃. Impedance research was conducted in the frequency range of 0.01 Hz to 1 MHz using a 0.01 mV AC signal amplitude. To ensure the materials were stable at their specified temperatures, the experimental conditions required a 30-minute holding period before evaluating each composition at each working temperature. The impedance spectra of YSC55, YSC64,

and YSC73 were analysed using two equivalent circuit models consisting of resistances R1 and R2, and constant phase elements CPE1 and CPE2. Figure 1 shows the equivalent circuit model used to analyse the impedance spectrum for YSC55, YSC64 and YSC73.

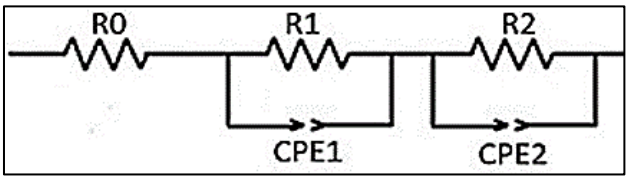

Fig. 1. Equivalent circuit for YSC55, YSC64 and YSC73

2.3 Porosity Testing

The process begins by preparing dry, well-sintered samples that meet specified standards. The study includes 12 YSZSDCC samples with composition ratios of 50:50, 60:40, and 70:30. Each sample is labelled with its composition and material type for easy grouping. The weights of all samples (W_D) are initially measured using a weighing machine. Subsequently, the samples are immersed in ethanol for an extended period of time to ensure complete saturation. Following the overnight soaking period, measure the weight of each sample while it is submerged to determine the soaking weight (W_S). Next, employ tissue to delicately absorb or eliminate surplus fluid from the sample prior to measuring the weight of the specimen when wet (W_W). The record weight was determined using the Eq. 1 for calculating the percentage apparent porosity.

$$\text{Percentage apparent porosity} = \frac{W_w - W_D}{W_{w-W_s}} \times 100 \times \rho \quad (1)$$

where W_D is the dry sample weight, W_w is the wet sample weight, W_S is the soak sample weight and ρ is the density of fluid (Ethanol = 0.785 g/cm^3).

3. Results

3.1 Phase Compatibility of YSZ-SDCC Composite Electrolyte Powders

XRD testing was conducted to identify the phase compatibility between YSZ commercial powder, and SDCC composite powders. Figure 2 shows that each composite electrolyte's XRD spectrum indicated the absence of secondary peaks or impurities following the milling process. The wet ball milling method and chosen calcination temperature are appropriate and do not interrupt the crystallite structure of YSZ-SDCC composites. The X-ray pattern of YSZ-SDCC composite cathode powders displays identical crystallite peaks to those of YSZ and SDC. SDC JCPDS pattern number is 01-075-0157. Once more, this demonstrates that only SDC exhibits a distinct fluorite crystal structure, while carbonates take on an amorphous structure. The study conducted by Mohamad *et al.,* [20] also identified the similar tendency. YSZ has s a JCPDS pattern number of 00-030-1468, featuring a face-centered cubic (FCC) lattice structure and belonging to the Fm3m space group. In an atomic arrangement structure, the FCC configuration includes an atom positioned at each of the eight corners and at the centre of each of the six faces, resulting in a closely packed structure. FCC material is often denser with a compact microstructure and exhibits stability at high temperatures because of its atomic packing arrangement [21].

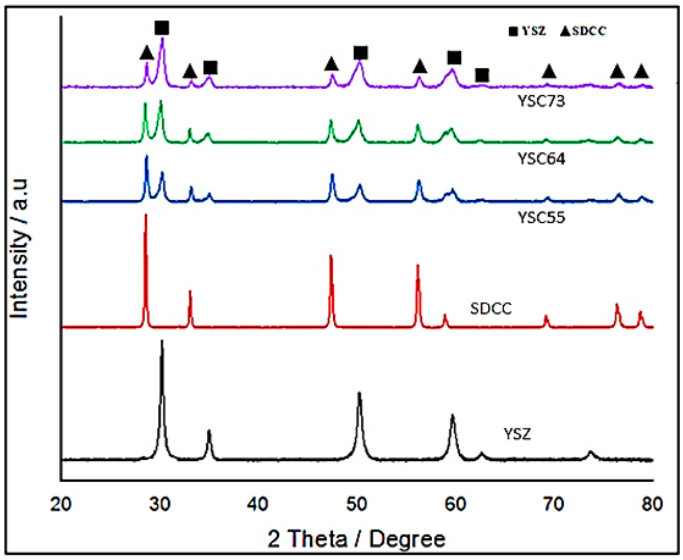

Fig. 2. XRD analysis for YSZ-SDCC composite electrolyte, commercial YSZ and SDC powder

3.2 FTIR Analysis of YSZ-SDCC Composite Electrolyte Powders

Due to the amorphous condition, XRD analysis did not detect the presence of carbonates. Therefore, FTIR spectroscopy was utilized to confirm the existence of carbonate bonding in the prepared YSZ-SDCC composite electrolyte. In Figure 3, the infrared spectra of commercial $(Li/Na)_2CO_3$, commercial SDC, and SDCC composite powder are displayed. Carbonate ions were identified in commercial $(Li/Na)_2CO_3$ at 1410 cm^{-1} and 1419 cm^{-1}. Minor peaks of carbonate ions were also identified at 860 cm^{-1} and 868 cm^{-1}. SDCC composite powder had peaks at 1430 cm^{-1} and 1506 cm^{-1}, indicating the presence of CO_3^{2-} bonds. Furthermore, small peaks of CO_3^{2-} bonds were identified at 860 cm^{-1}. Carbonate bonds were detected between 1500 cm^{-1} and 1410 cm^{-1} by Hoa *et al.,* [22] and Bakar *et al.,* [23]. The investigation of carbonate bonding was conducted using the infrared band database provided by the National Institute of Standards and Technology (NIST).

The presence of the CO_3^{2-} phase on YSZ-SDCC is essential in order to maintain carbonate elements in the composite powder after undergoing milling with YSZ electrolyte. Figure 4 displays the FTIR spectra of SDCC, YSZ-SDC and prepared YSZ-SDCC composite powders in the three distinct compositions. As expected, the carbonates bond was not detected in the YSZ-SDC composite powder sample. The YSZ-SDCC composite powders exhibited peaks corresponding to carbonate bonds in the spectral region of 1430-1520 cm^{-1} and 866 cm^{-1}. The functional groups of carbonate ions are found at wavenumbers of 1490 cm^{-1} to 1410 cm^{-1} and 880 cm^{-1} to 860 cm^{-1} [24]. The peak in the 1430-1520 cm^{-1} range exhibited stretching and expanding modes in comparison to the second region. The first absorption in infrared analysis is commonly strong and wide. Conversely, the second absorption is of low to moderate strength and results in a narrow peak [24].

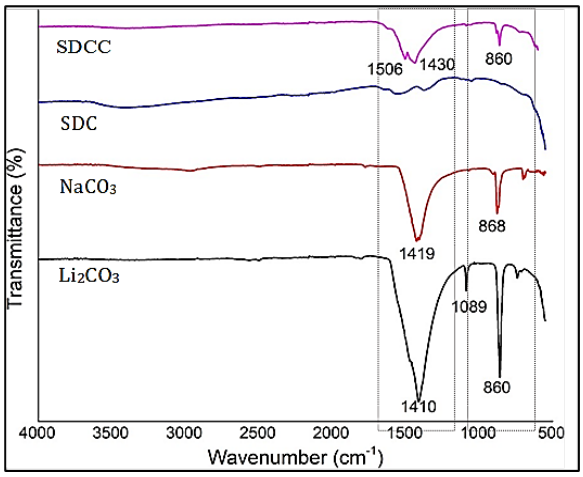

Fig. 3. The infrared spectra of commercial SDC, commercial $(Li/Na)_2CO_3$ and SDCC composite powders

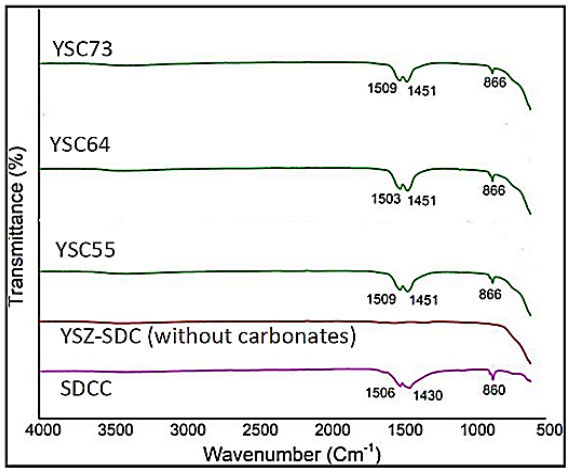

Fig. 4. FTIR spectra of YSZ-SDCC composite cathode at three different compositions

3.3 Particle Morphology Analysis and Element Distribution Of YSZ-SDCC Composite Electrolytes Powders

The powder morphology and elemental distribution of YSZ-SDCC composite electrolytes powders with three compositions were investigated. The morphology of YSZ-SDCC composite electrolytes powders with different ratios of YSZ and SDC is portrayed in Figures 5(a) to 5(c). The morphology of the particles displays a highly detailed structure. Observing some mild clumping among the particles. Prior to milling and calcining, the particle sizes of the commercial YSZ and SDC powders were 379 nm and 130 nm, respectively. Following the milling and calcination procedure, YSZ-SDCC composite cathode powders exhibit consistent particle sizes that are less than 300 nm. The Image J software was utilized to calculate the average particle size of all the produced powders obtained via FESEM micrograph examination.

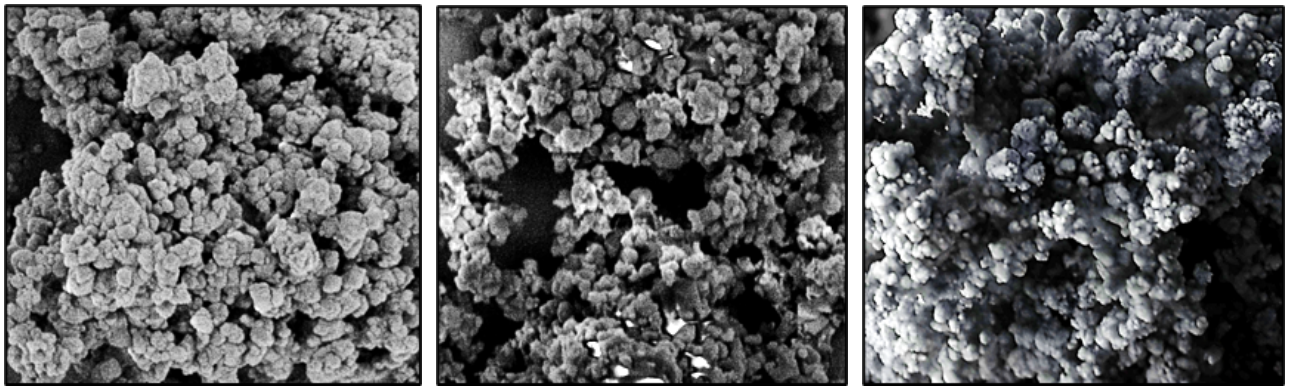

(a) (b) (c)

Fig. 5. FESEM micrograph of composite electrolyte powders (a) YSC55 (b) YSC64 (c) YSC73

Table 2 shows the average particle size for YSZ-SDCC composite electrolytes powders. The results show that YSC73 has the smallest particles sizes, followed by YSC55 and YSC64. The composite powders' particle size of 100-200 nm was advantageous since it reduced the particle size and improved the surface area. This scenario will expand the triple phase boundary (TPB) area for the oxygen reduction reaction in cathode components, leading to improved cell performance [25,26]. The investigation of particle size for the YSZ-SDCC composite cathode indicates that variations in

composition of the manufactured composite powders do not have a major impact on their particle size. Figure 6 shows the EDS spectra of YSZ-SDCC composite electrolytes powders after milling at 550 rpm for 2 hours.

Table 2
Average particles sizes for YSZ-SDCC composites electrolytes powders

Samples	Average particle size (nm)
YSC55	244.97 ± 40.66
YSC64	213.47 ± 41.63
YSC73	173.27 ± 25.83

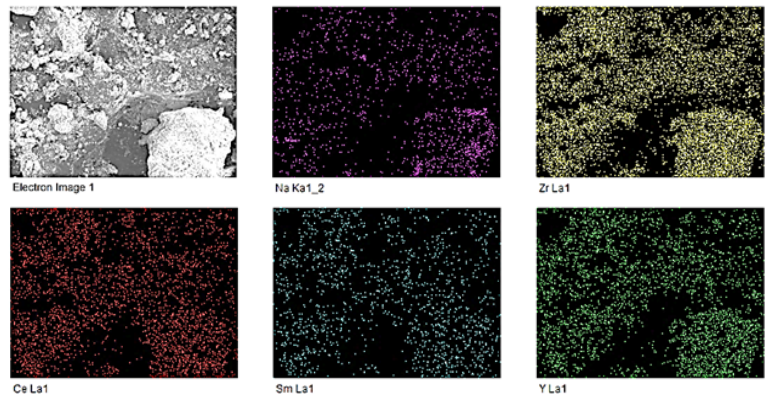

(a)

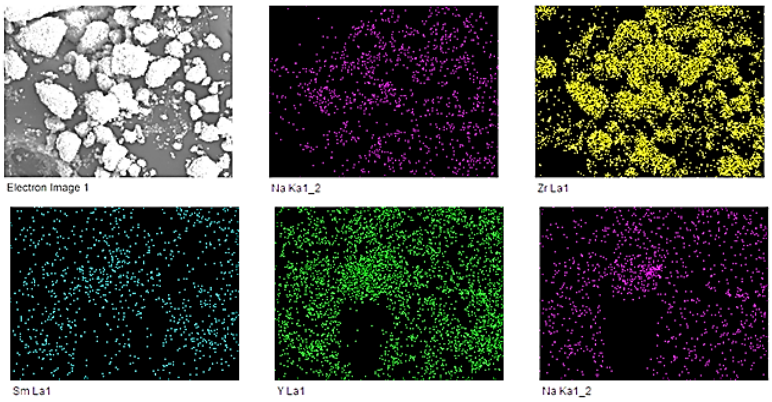

(b)

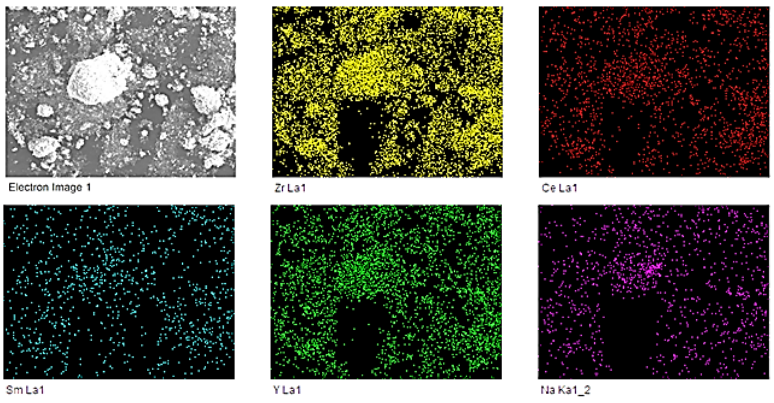

(c)

Fig. 6. EDS spectra (a) YSC55 (b) YSC64 (c) YSC73

According to Figure 6, all elements in the mixed YSZ-SDCC powders such as yttrium (Y), zirconia (Zr), samarium (Sm), cerium (Ce), and sodium (Na) were homogenously and well distributed. The HEBM method contributed to the production of a uniform and evenly distributed YSZ-SDCC composite electrolyte powder. However, the absence of lithium (Li) detection can be attributed to its low scanning X-ray energy band and low atomic mass [26]. Another important thing to keep in mind is that following the milling process, homogeneity and evenly distributed elements are crucial for extending the triple phase boundary (TPB), which helps to complete catalytic activity and improve electrochemical performances [27].

3.4 Electrochemical Performances of YSZ-SDCC Symmetrical Cell

Nyquist plot was constructed, and impedance values (Z value) were determined from the plotted graph. Figures 7(a) to 7(c) shows the Nyquist plots for the symmetrical cell of YSZ-SDCC at three different operating temperatures. The ionic conductivity was determined using the Rp data extracted from the impedance graph. Rp is the total of R1 and R2. Table 3 displays the calculated ionic conductivity and Rp values for YSC55, YSC64 and YSC73. Total conductivity was calculated using the equation from Eq. 2.

$$\sigma = \frac{1}{\rho} = \left(\frac{1}{R}\right) \times \left(\frac{l}{S}\right) \tag{2}$$

where ρ is the resistivity (Ω.m), R is the total resistance of Rp values (Ω), l and S is the thickness of the sample (cm) and the effective area of the sample (cm^2).

Figure 7 displays Nyquist plots illustrating a decrease in impedance curves' resistance as the operating temperature rises from 500℃ to 700℃. At 700 ℃, YSC55 gives the lowest resistance followed by YSC64 and YSC73. This demonstrates that a higher carbonate ratio helps to improve the electrochemical performance of the symmetrical cell. As seen in Table 3, the measured ionic conductivity was significantly low. The desired high ionic conductivity for the ideal fuel cell operation at low temperatures typically falls within the range of 0.001-0.1 Scm^{-1} [28]. The highest ionic conductivity achieved in this investigation was with YSC55, followed by YSC64 and YSC73, with conductivity values of 0.009 Scm^{-1}, 0.005 Scm^{-1} and 0.0004 Scm^{-1} respectively. The variations in conductivity in YSZ-SDCC were due to changes in carbonate concentration among the samples. YSC55 exhibits the best conductivity at 700 degrees due to its higher SDCC concentration compared to YSC64 and YSC73. Jing *et al.,* [29] demonstrated that the ionic conductivity increases when the concentration of carbonate salt is increased in the combination with SDC. Rahman *et al.,* [30] also discovered that a composite cathode containing 50% SDCC concentration (the highest carbonate percentage) had superior cell performance compared to other ratios. Additionally, the electrochemical performance of YSC55, YSC64 and YSC73 was calculated using area specific resistance (ASR) formula in Eq. 3. The ASR values for YSC55 at 700℃ are the smallest (8.79 Ω cm^2) compared to YSC64 (14.65 Ω cm^2) and YSC73 (186.22 Ω cm^2).

$$ASR = (R_p \times S)/2 \tag{3}$$

where R_p is polarisation resistance (Ω) and S the effective area of the sample (cm^2).

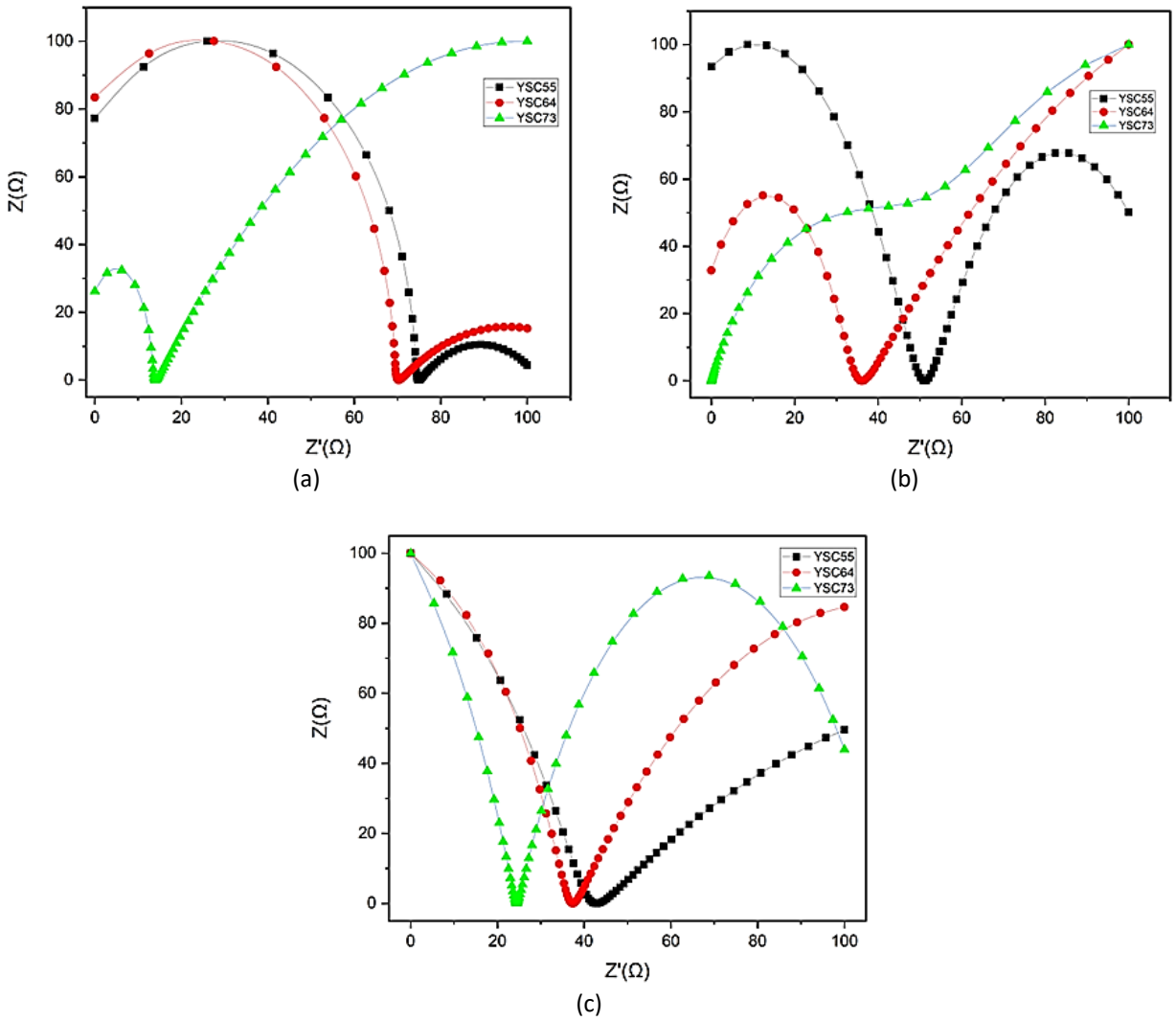

Fig. 7. Nyquist plot for YSC55, YSC64 and YSC73 (a) 700 ℃ (b) 600 ℃ (c) 500℃

Table 3
Electrochemical performances of YSC55, YSC64 and YSC73 at 500℃-700℃

Temperature (℃)	Samples	Total resistance (R_P) [Ω]	Conductivity, (σ) [$\times \mathbf{10^{-3}} S\ cm^{-1}$]	ASR [Ω cm^2]
700	YSC55	13.24	9.0	8.79
	YSC64	22.07	5.0	14.65
	YSC73	280.6	0.4	186.22
600	YSC55	38.00	3.0	25.22
	YSC64	59.26	2.0	39.33
	YSC73	612.00	0.1	406.16
500	YSC55	404.00	0.3	268.12
	YSC64	294.00	0.4	195.12
	YSC73	1450.00	0.07	962.31

A further analysis of the porosity of YSC55, YSC64, and YSC73 is also being carried out as part of this study. Porosity is an essential attribute that can impact the physical, mechanical, and thermal traits of a material. Pores impact characteristics including density, strength, permeability, and thermal conductivity. One important consideration is the relationship between the powder's particle size and the samples' porosity. It is evident that the sample with the highest porosity is the one with the lowest particle size. YSC73 has the smallest average particle size of 173.27 ± 25.83 nm compared to YSC64 and YSC55. Smaller particle sizes exhibit greater porosity, with YSC73 showing a porosity of

39%. Small particles are prone to agglomeration, leading to a reduction in the rate of body compaction and particle development during the pellet sintering process. The calculated porosity for YSC55, YSC64 and YSC73 was from Eq. 3 and summarized in Table 4.

Table 4
Average porosity for YSC55, YSC64 and YSC73

Samples	Apparent porosity (%)
YSC55	34.43 ±0.72
YSC64	36.72 ±0.72
YSC73	39.62 ±0.72

4. Conclusions

In conclusion, the findings from this study mark a notable step forward particularly in the exploration of composite electrolytes involving YSZ-SDCC. The results of phase identification, carbonate analysis, morphological microstructural, and electrochemical performances of YSC-SDCC composite electrolytes and YSZ-SDCC symmetrical cells at 3 distinct compositions were thoroughly examined and confirmed. YSC55, YSC64 and YSC73 successfully maintained their lattice structure without the presence of impurity after the milling process. This investigation showed that the composition ratio of YSZ-SDCC composite had a modest impact on the particle size, elemental distribution, surface area, porosity, and polarization resistance of composite electrolytes. The present study shows that a higher ratio of binary carbonate in composite electrolytes enhances the performance of electrochemical cells. The composite electrolytes are made of 50wt.% YSZ and 50wt.% SDCC was determined to be the most promising composition in this study. Although the ionic conductivity and polarization resistance of YSC55, YSC64, and YSC73 are currently not within the desired range, there is still potential to improve with further evaluation of physical, chemical, mechanical, and electrochemical properties

Acknowledgement
The research was supported by Universiti Tun Hussein Onn Malaysia (UTHM) through Tier 1 (vot Q494) and Postgraduate Research Grant, REGG (vot Q205).

References
[1] Veerendra, Arigela Satya, Kumaran Kadirgama, Norazlianie Sazali, Sivayazi Kappagantula, and Subbarao Mopidevi. "An MPPT controller with a modified four-leg interleaved DC/DC boost converter for fuel cell applications." *Journal of Advanced Research in Applied Sciences and Engineering Technology* 53, no. 1 (2024): 219-236. https://doi.org/10.37934/araset.53.1.219236

[2] Baharuddin, Nurul Akidah, Nurul Farhana Abdul Rahman, Hamimah Abd. Rahman, Mahendra Rao Somalu, Mohd Azham Azmi, and Jarot Raharjo. "Fabrication of high-quality electrode films for solid oxide fuel cell by screen printing: A review on important processing parameters." *International Journal of Energy Research* 44, no. 11 (2020): 8296-8313. https://doi.org/10.1002/er.5518

[3] Mendonça, Catarina, António Ferreira, and Diogo MF Santos. "Towards the commercialization of solid oxide fuel cells: recent advances in materials and integration strategies." *Fuels* 2, no. 4 (2021): 393-419. https://doi.org/10.3390/fuels2040023

[4] Haghghi, Maghsoud Abdollahi, Shahriyar Ghazanfari Holagh, Ata Chitsaz, and Kiyan Parham. "Thermodynamic assessment of a novel multi-generation solid oxide fuel cell-based system for production of electrical power, cooling, fresh water, and hydrogen." *Energy Conversion and Management* 197 (2019): 111895. https://doi.org/10.1016/j.enconman.2019.111895

[5] Weber, Adam Z., and Timothy E. Lipman. "Fuel cells and hydrogen production: introduction." In *Fuel Cells and Hydrogen Production*, p. 1-8. Springer, New York, NY, 2019. https://doi.org/10.1007/978-1-4939-7789-5_1051

[6] Dwivedi, Sudhanshu. "Solid oxide fuel cell: Materials for anode, cathode and electrolyte." *International Journal of Hydrogen Energy* 45, no. 44 (2020): 23988-24013. https://doi.org/10.1016/j.ijhydene.2019.11.234
[7] Corigliano, Orlando, Leonardo Pagnotta, and Petronilla Fragiacomo. "On the technology of solid oxide fuel cell (SOFC) energy systems for stationary power generation: A review." *Sustainability* 14, no. 22 (2022): 15276. https://doi.org/10.3390/su142215276
[8] Choudhury, Arnab, H. Chandra, and A. Arora. "Application of solid oxide fuel cell technology for power generation A review." *Renewable and Sustainable Energy Reviews* 20 (2013): 430-442. https://doi.org/10.1016/j.rser.2012.11.031
[9] Naeini, Mina, James S. Cotton, and Thomas A. Adams. "Economically optimal sizing and operation strategy for solid oxide fuel cells to effectively manage long-term degradation." *Industrial & Engineering Chemistry Research* 60, no. 47 (2021): 17128-17142. https://doi.org/10.1021/acs.iecr.1c03146
[10] Solovyev, A. A., A. V. Shipilova, S. V. Rabotkin, N. M. Bogdanovich, and E. Yu Pikalova. "Study of the efficiency of composite $LaNi_{0.6}$ $Fe_{0.4}$ O_3-based cathodes in intermediate-temperature anode-supported SOFCs." *International Journal of Hydrogen Energy* 48, no. 59 (2023): 22594-22609. https://doi.org/10.1016/j.ijhydene.2023.02.011
]11] Wachsman, Eric D., and Kang Taek Lee. "Lowering the temperature of solid oxide fuel cells." *Science* 334, no. 6058 (2011): 935-939. https://doi.org/10.1126/science.1204090
[12] Fergus, Jeffrey, Rob Hui, Xianguo Li, David P. Wilkinson, and Jiujun Zhang. *Solid oxide fuel cells: materials properties and performance*. CRC press, 2016. https://doi.org/10.1201/9781420088847
[13] Cheng, Jigui, Qiumei Jiang, Haigen He, Junfang Yang, Yifang Wang, and Jianfeng Gao. "Preparation and characterization of Y_2O_3–Sm_2O_3 co-doped ceria electrolyte for IT-SOFCs." *Materials Chemistry and Physics* 125, no. 3 (2011): 704-708. https://doi.org/10.1016/j.matchemphys.2010.09.070
[14] Matsui, Toshiaki, Siqi Li, Hiroki Muroyama, Kyosuke Kishida, Haruyuki Inui, and Koichi Eguchi. "Electrochemical property of solid solutions formed in (La, Sr)(Co, Fe) O_3− δ cathode/doped-CeO2 interlayer/Y_2O_3–ZrO_2 electrolyte system during operation of solid oxide fuel cells." *Solid State Ionics* 300 (2017): 135-139. https://doi.org/10.1016/j.ssi.2016.12.014
[15] Spiridigliozzi, Luca. *Doped-Ceria Electrolytes: Synthesis, Sintering and Characterization*. Springer, 2018. https://doi.org/10.1007/978-3-319-99395-9
[16] Kilner, John A., and Monica Burriel. "Materials for intermediate-temperature solid-oxide fuel cells." *Annual Review of Materials Research* 44 (2014): 365-393. https://doi.org/10.1146/annurev-matsci-070813-113426
[17] Fan, Liangdong, Chuanxin He, and Bin Zhu. "Role of carbonate phase in ceria–carbonate composite for low temperature solid oxide fuel cells: a review." *International Journal of Energy Research* 41, no. 4 (2017): 465-481. https://doi.org/10.1002/er.3629
[18] Rahman, Hamimah Abdul, Linda Agun, and Mohamed Hakim Ahmad Shah. "Ba-and La-strontium cobalt ferrite carbonate composite as cathode materials for low temperature SOFC." *Key Engineering Materials* 694 (2016): 125-129. https://doi.org/10.4028/www.scientific.net/KEM.694.125
[19] Hoa, N. K., H. A. Rahman, and M. R. Somalu. "Effects of NiO loading and pre-calcination temperature on NiO-SDCC composite anode powder for low-Temperature solid oxide fuel cells." *Ceramics-Silikaty* 62, no. 1 (2018): 50-58. https://doi.org/10.13168/cs.2017.0044
[20] Mohammad, Siti Fairus, Sufizar Ahmad, Hamimah Abdul Rahman, and Andanastuti Muchtar. "Effect of SSC loading on the microstructural stability SSC-SDCC composite cathode as new potential SOFC." *International Journal of Integrated Engineering* 11, no. 7 (2019): 162-168. https://doi.org/10.30880/ijie.2019.11.07.021
[21] Wu, Zhenggang, Hongbin Bei, George M. Pharr, and Easo P. George. "Temperature dependence of the mechanical properties of equiatomic solid solution alloys with face-centered cubic crystal structures." *Acta Materialia* 81 (2014): 428-441. https://doi.org/10.1016/j.actamat.2014.08.026
[22] Hoa, Ng Kei, Hamimah Abd Rahman, and Mahendra Rao Somalu. "Influence of silver addition on the morphological and thermal characteristics of nickel oxide-samarium doped ceria carbonate (NiO-SDCC) Composite Anode." *International Journal of Integrated Engineering* 10, no. 1 (2018): 196-201. https://doi.org/10.30880/ijie.2018.10.01.030
[23] Bakar, Mohd Subri Abu, Sufizar Ahmad, Siti Fairus Mohammad, and Hamimah Abdul Rahman. "Characteristics of Ag element on LSCF-SDCC-Ag composite cathode for LTSOFC potential applications." *Journal of Advanced Mechanical Engineering Applications* 1, no. 1 (2020): 20-26. https://doi.org/10.30880/jamea.2020.01.01.003
[24] Coates, John. "Interpretation of infrared spectra, a practical approach." *Encyclopedia of Analytical Chemistry* 12 (2000): 10815-10837. https://doi.org/10.1002/9780470027318.a5606
[25] Bakar, M. S. A., H. A. Rahman, S. F. Mohammad, S. Ahmad, and A. Muchtar. "Morphological and physical behaviour of LSCF-SDCC-Ag composite cathode with the incorporation of Ag as an additive element." In *Journal of Physics: Conference Series*, 914, no. 1, p. 012011. IOP Publishing, 2017. https://doi.org/10.1088/1742-6596/914/1/012011

[26] Sun, Yifei, Ning Yan, Jianhui Li, Huayi Wu, Jing-Li Luo, and Karl T. Chuang. "The effect of calcination temperature on the electrochemical properties of $La_{0.3}Sr_{0.7}Fe_{0.7}Cr_{0.3}O_3$ − x (LSFC) perovskite oxide anode of solid oxide fuel cells (SOFCs)." *Sustainable Energy Technologies and Assessments* 8 (2014): 92-98. https://doi.org/10.1016/j.seta.2014.08.001

[27] Khan, Ieeba, Muhammad Imran Asghar, Peter D. Lund, and Suddhasatwa Basu. "High conductive $(LiNaK)_2CO_3Se_{0.85}Sm_{0.15}O_2$ electrolyte compositions for IT-SOFC applications." *International Journal of Hydrogen Energy* 42, no. 32 (2017): 20904-20909. https://doi.org/10.1016/j.ijhydene.2017.05.152

[28] Zakaria, Zulfirdaus, Saiful Hasmady Abu Hassan, Norazuwana Shaari, Ahmad Zubair Yahaya, and Yap Boon Kar. "A review on recent status and challenges of yttria stabilized zirconia modification to lowering the temperature of solid oxide fuel cells operation." *International Journal of Energy Research* 44, no. 2 (2020): 631-650. https://doi.org/10.1002/er.4944

[29] Jing, Yifu, Janne Patakangas, Peter D. Lund, and Bin Zhu. "An improved synthesis method of ceria-carbonate based composite electrolytes for low-temperature SOFC fuel cells." *International Journal of Hydrogen Energy* 38, no. 36 (2013): 16532-16538. https://doi.org/10.1016/j.ijhydene.2013.05.136

[30] Rahman, Hamimah Abd, Andanastuti Muchtar, Norhamidi Muhamad, and Huda Abdullah. "Structure and thermal properties of $La_{0.6}Sr_{0.4}Co_{0.2}Fe_{0.8}O_{3-\delta}$–SDC carbonate composite cathodes for intermediate-to low-temperature solid oxide fuel cells." *Ceramics International* 38, no. 2 (2012): 1571-1576. https://doi.org/10.1016/j.ceramint.2011.09.043